Spectroscopy of $LiYF_4:Eu^{3+}$ single crystals

1990 J. Phys.: Condens. Matter 2 5703

(http://iopscience.iop.org/0953-8984/2/26/006)

J. Phys.: Condens. Matter **2** (1990) 5703–5713. Printed in the UK

Spectroscopy of $LiYF_4:Eu^{3+}$ single crystals

Bipin Bihari†, K K Sharma† and L E Erickson‡

† Department of Physics and Centre for Laser Technology, Indian Institute of Technology, Kanpur 208 016, India

‡ National Research Council of Canada, Ottawa K1A 0R8, Canada

Received 15 January 1990

Abstract. Polarised absorption and laser-induced fluorescence spectra of $LiYF_4:Eu^{3+}$ were recorded at liquid-nitrogen temperature in the visible spectral range. Transitions with pure electric dipole, pure magnetic dipole and mixed dipolar character have been observed. Spectroscopic assignments to the energy levels are made on the basis of the observed energies, polarisation characteristics of the spectral lines and electric and magnetic dipole selection rules relevant to the S_4 point group. 37 Stark components belonging to ten multiplets of Eu^{3+} have been established. Free-ion and crystal-field parameters have been obtained. Simulation of the crystal-field energy levels has been attempted with and without J–J mixing effects using intermediate-coupling wavefunctions.

1. Introduction

Trivalent europium is unique among rare-earth ions in that it has a ground state with total angular momentum $J = 0$. There are strong selection rules which forbid transitions from this ground state to many of the excited states. In particular, the $J = 0 \rightarrow 0$ transition is forbidden in electric dipole (ED) and magnetic dipole (MD) approximations and, further, the normally allowed 'forced electric dipole' transitions in rare-earth ions in a crystalline environment are also not permitted from $J = 0$ states to odd-J states. As a consequence of these selection rules, the $^7F_0$–$^5D_0$ transition is seldom observed in absorption or emission. Similarly, the $^7F_0$–$^5D_3$ and the weakly observed $^7F_0$–$^5D_1$ and $^5D_0$–$^7F_3$, $^7F_5$ transitions are in general agreement with these selection rules. The crystal-field effects leading to mixing of pure J states allow these transitions to be weakly observed. $LiYF_4:Eu^{3+}$ is one of the few examples where the existence of magnetic dipole transitions in the optical spectrum has been unambiguously established. The $^7F_0$–$^5D_1$ transition of Eu^{3+} in the S_4 site symmetry of $LiYF_4$ is not permitted in the ED approximation but is permitted in the MD approximation. The experimental observations are in complete agreement with this fact [1]. This ion–host combination with a non-degenerate ground state is particularly useful for optically detected nuclear magnetic resonance studies [2]. At the same time, the system with six electrons in the 4f shell is sufficiently complex for the interpretation of its optical spectrum. In the only other published work on this system, Görller-Walrand *et al* [3] have analysed fluorescence from $^5D_{0,1}$ multiplets to some of the ^7F_J multiplets. Our measurements involving absorption, excitation spectrum and laser-induced fluorescence cover some additional multiplets. Further, our detailed polarisation measurements have allowed us to use the exact site

0953-8984/90/265703 + 11 $03.50

symmetry S_4. We have identified several vibronic transitions which were helpful in making symmetry assignments [1]. The crystal-field parameters in [3] were obtained by considering J–J mixing within the ^7F_J multiplets. We have attempted to describe the crystal-field effects within ^7F and ^5D multiplets with and without J–J mixing effects using intermediate-coupling wavefunctions. Because of computational constraints, it was necessary to adopt a truncation procedure while considering the J–J mixing effects.

2. Crystal structure and experimental details

The uniaxial $LiYF_4$ single crystal is isomorphous to scheelite-type crystals such as $CaWO_4$ having a tetragonal crystal structure [4] (space group C_{4h}^6) with $a = b = 5.26$ Å, $c = 10.94$ Å and $\alpha = \beta = \gamma = 90°$. Eight F^- ions surrounding the Y^{3+} ion form a poly-

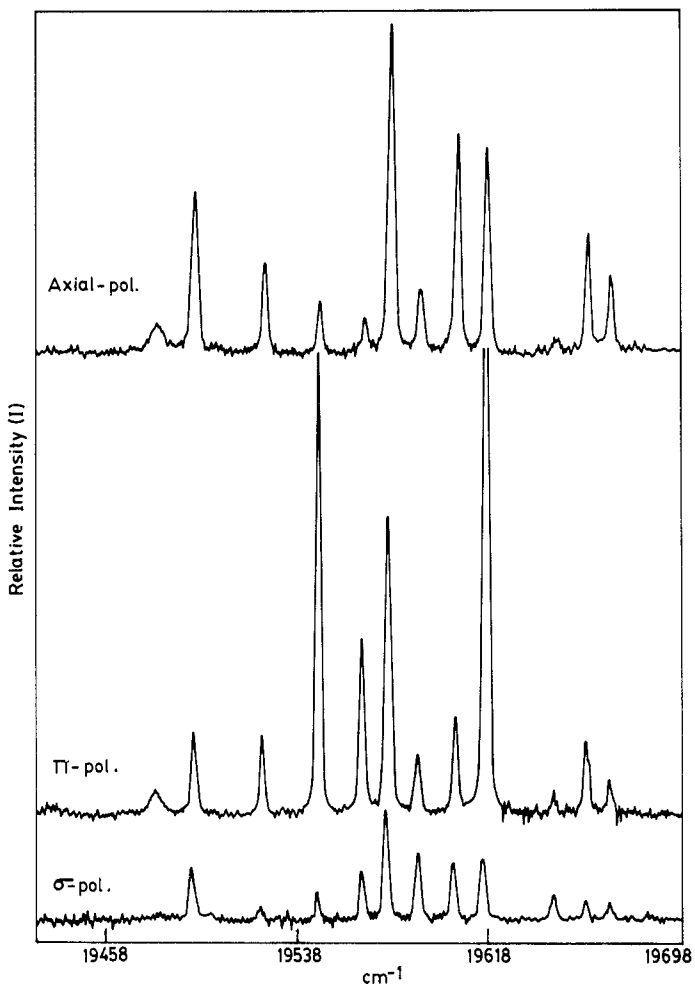

Figure 1. $^5D_2$–$^7F_3$ fluorescence of $LiYF_4$: Eu^{3+} at liquid-nitrogen temperature.

hedron which is nearly a dodecahedron. In the absence of F^- ions, site symmetry at the position of the Y^{3+} ion would be D_{2d}. The presence of F^- lowers the symmetry to S_4. The $LiYF_4$ presents a tight structure and, on doping, rare-earth ions are unlikely to be found in the interstitial positions. The oriented and cut sample used in the present study measured 3.8 mm × 2.1 mm × 3.1 mm with the crystallographic $\bar{c}$ axis parallel to the 3.1 mm edge. The Eu^{3+} concentration in the sample was about 1%.

Spectroscopic measurements were made using a Carl–Zeiss double-grating monochromator model GDM-1000 which has a resolution of better than 0.5 cm^{-1} in the range of our investigation. For absorption measurements, a water-cooled 1000 W tungsten–halogen lamp and, for recording the fluorescence and excitation spectra, a 15 W Coherent Ar^+ laser and a coherent ring dye laser were used. The sample was cooled to liquid-nitrogen temperature. All spectra were recorded in π, σ and axial modes. Figure 1 shows a typical spectrum corresponding to $^5D_2$–$^7F_3$ fluorescence. In order to compensate for the polarisation characteristics of the monochromator, the spectral profile of the tungsten–halogen lamp was recorded by inserting the sheet polariser between the lamp and the entrance slit of the monochromator in σ and π orientations and the necessary correction factors obtained in the region of our interest.

The $LiYF_4:Eu^{3+}$ exhibits fluorescence when excited with most of the Ar-ion laser lines, although excitation in all cases is non-resonant. The $^5D_2$ excitation produces fluorescence from $^5D_2$, $^5D_1$ and $^5D_0$ multiplets as well, while $^5D_1$ excitation produces fluorescence from $^5D_1$ and $^5D_0$ multiplets. Since the $^7F_0$–$^5D_0$ transition is restricted by several selection rules, its resonance excitation using the dye laser was also not very effective. However, the excitation spectrum obtained by monitoring $^5D_0(\Gamma_1)$–$^5F_1(\Gamma_1)$ fluorescence transition at 16 842 cm^{-1} and scanning the dye laser from 16 900–17 800 cm^{-1} shows that the $^5D_0$ level can be excited quite efficiently with the dye laser lasing at 16 938 cm^{-1} (which corresponds to the wavenumber interval for the $^7F_1(\Gamma_3)$–$^5D_0(\Gamma_1)$ transition) and at 17 630 cm^{-1} (phonon-assisted excitation).

3. Spectroscopic assignments

The Stark levels of Eu^{3+} in $LiYF_4$ can be characterised by four irreducible representations Γ_1, Γ_2, Γ_3 and Γ_4 (as Γ_3 and Γ_4 are degenerate, they are denoted by Γ_3) of the symmetry group S_4 [5]. Spectroscopic assignments to energy levels were made on the basis of the observed energies, polarisation characteristics of transitions between them and the selection rules for ED and MD transitions (table 1). Lines with comparable intensities in σ (π) and axial spectra are associated with ED (MD) transitions. Mixed (ED

Table 1. Forced ED and MD selection rules for the S_4 site symmetry in $LiYF_4:Eu^{3+}$.

	ED				MD			
	Γ_1	Γ_2	Γ_3	Γ_4	Γ_1	Γ_2	Γ_3	Γ_4
Γ_1	—	π	σ	σ	σ	—	π	π
Γ_2	π	—	σ	σ	—	σ	π	π
Γ_3	σ	σ	π	—	π	π	—	σ
Γ_4	σ	σ	—	π	π	π	σ	—

and MD) transitions appear in both σ and π polarisations. The criteria used to decide dominant nature of mixed transitions are

$$I_\pi < I_\sigma < I_{ax} \rightarrow \sigma\text{-ED (dominant)}, \pi\text{-MD}$$
$$I_\sigma < I_\pi < I_{ax} \rightarrow \pi\text{-MD (dominant)}, \sigma\text{-ED}$$
$$I_\sigma > I_\pi > I_{ax} \rightarrow \sigma\text{-MD (dominant)}, \pi\text{-ED}$$
$$I_\pi > I_\sigma > I_{ax} \rightarrow \pi\text{-ED (dominant)}, \sigma\text{-MD}.$$

From our data, we have been able to establish the structure of ^5D_J ($J = 0$–2) and ^7F_J ($J = 0$–4) multiplets completely, while the structure of $^7F_5$ and $^5L_6$ multiplets could be established only partially.

3.1. ^5D multiplets

The $^7F_0(\Gamma_1)$–$^5D_0(\Gamma_1)$ energy level separation has been reported to be 17 263 cm^{-1} at liquid-helium temperature and 17 270 cm^{-1} at liquid-nitrogen temperature [2, 3]. We have not observed this transition at 77 K but our fluorescence data put the $^5D_0(\Gamma_1)$ level at 17 271 cm^{-1}. The two magnetic dipole transitions observed at 19 021 and 19 043 cm^{-1} in the absorption spectrum are assigned to the $^7F_0(\Gamma_1)$–$^5D_1(\Gamma_3)$ and $^7F_0(\Gamma_1)$–$^5D_1(\Gamma_1)$ transitions, respectively. The observed fluorescence from the $^5D_1$ multiplet to various ^7F_J multiplets is consistent with this assignment.

The $^5D_2$ multiplet splits into four components: Γ_1, two Γ_2 and Γ_3 [5]. Three ED transitions at 21 450, 21 520 and 21 543 cm^{-1} observed in the absorption spectrum establish the positions of $\Gamma_2(1)$, Γ_3 and $\Gamma_2(2)$ components of this multiplet. The $^5D_2$–$^7F_0$ fluorescence in the spectral range 21 400–21 570 cm^{-1} confirms this assignment. The position of the remaining $^5D_2(\Gamma_1)$ level was inferred from the $^5D_2$–$^7F_1$ fluorescence. The fairly strong σ-ED and somewhat weaker π-MD line observed at 21 145 cm^{-1} for this fluorescence group is assigned to the $^5D_2(\Gamma_1)$–$^7F_1(\Gamma_3)$ transition, suggesting the $^5D_2(\Gamma_1)$ Stark level at 21 479 cm^{-1}. This multiplet was established for the first time. However, we could not observe any transition involving $^5D_3$ multiplet.

3.2. $^5L_6$ multiplet

Four fairly strong and well separated lines at 25 416, 25 241, 25 027 and 24 953 cm^{-1} and a broad shoulder at 25 258 cm^{-1} associated with the 25 241 cm^{-1} line are present in the spectral region 24 900–25 500 cm^{-1} of the absorption spectrum. A literature survey and our free-ion calculations [1, 6] indicate that the $^5D_3$, $^5L_6$ and $^5G_2$ multiplets lie in the ranges 24 300–24 500 cm^{-1}, 24 900–25 400 cm^{-1} and 25 900–26 100 cm^{-1}, respectively. The above-observed spectral lines are thus associated with $^7F_0$–$^5L_6$ transitions. This multiplet should have ten Stark components: three Γ_1, four Γ_2 and three Γ_3. It is reasonable to expect Γ_1–Γ_1 transitions not to appear for this group as MD transitions are forbidden for $\Delta J > \pm 1$. We assign the σ-ED lines at 24 953 and 25 241 cm^{-1} to the Γ_1–Γ_3 transitions and the π-ED line at 25 027 cm^{-1} to the Γ_1–Γ_2 transition, thus establishing the positions of the $\Gamma_3(1)$, $\Gamma_3(2)$ and $\Gamma_2(1)$ components of $^5L_6$. The broad shoulder is σ-ED type, but our theoretical calculations do not support a Γ_3 level at this energy. This line is left unassigned. The line at 25 416 cm^{-1} is strong and very broad (FWHM, 34 cm^{-1}). Its peak positions in π- and σ-polarised spectra differ by 3 cm^{-1} and the peak in the axial

spectra matches that of the σ-polarisation. We therefore believe this line to consist of two lines: the π-ED peak at 25 418 cm^{-1} is assigned to the Γ_1–$\Gamma_2(2)$ and the σ-ED peak at 25 415 cm^{-1} to the Γ_1–$\Gamma_3(3)$ transitions. Thus, out of ten expected Stark levels of $^5L_6$, five are identified. These assignments are in qualitative agreement with the calculated structure of the $^5L_6$ multiplet. However, the complete identification of this multiplet was not possible.

3.3. ^7F multiplets

The ^7F_J multiplets with $J = 0$–6 lie in the spectral range 0–5500 cm^{-1}. Their structure can be derived from a systematic analysis of the fluorescence originating from the ^5D_J multiplets. Fluorescence measurements were made by irradiating the sample with 457.9 and 514.5 nm lines of the Ar^+ laser or with the dye laser tuned to excite the $^5D_0$ level. The extensive fluorescence observed from the $^5D_0$, $^5D_1$ and $^5D_2$ multiplets to the Stark levels of the ^7F_J multiplets was helpful in cross checking the symmetry assignments of the ^5D_J and ^7F_J multiplets. Our assignments for these multiplets are in general agreement (within ± 3 cm^{-1}) with those of Görller *et al* [3]. However, there are differences in the details of assignment arising most probably from the non-availability of complete polarisation information in [3]. For example, the 17 868 cm^{-1} line has been assigned [3] to the σ-MD, $^5D_1(\Gamma_1)$–$^7F_2(\Gamma_1)$ transition, while the mixed (π-MD dominant plus σ-ED) character observed by us suggests that this line corresponds to the $^5D_1$ (Γ_3)–$^7F_2(\Gamma_2(2))$ transition. Similarly, the $^5D_1$–$^7F_5$ fluorescence lines at 15 245 cm^{-1}, 15 236 cm^{-1} and 15 223 cm^{-1} were assigned to the Γ_1–Γ_2, Γ_1–Γ_3 and Γ_3–Γ_2 transitions in [3], giving the positions of the $\Gamma_2(1)$ and $\Gamma_3(1)$ levels of the $^7F_5$ multiplet at 3795 cm^{-1} and 3807 cm^{-1}, respectively, whereas we find the Γ_1–$\Gamma_3(1)$, Γ_3–$\Gamma_2(1)$ and Γ_3–$\Gamma_3(1)$ assignments more appropriate for these lines, thus establishing the $\Gamma_2(1)$ and $\Gamma_3(1)$ levels of $^7F_5$ at 3786 cm^{-1} and 3799 cm^{-1}, respectively. The Stark levels $^7F_4(\Gamma_1(3))$ (3081 cm^{-1}), $^7F_5(\Gamma_1(1))$ (3844 cm^{-1}) and $^7F_5(\Gamma_1(2))$ (4008 cm^{-1}) have been identified for the first time. Two sharp and rather strong lines in the $^5D_0$–$^7F_1$ fluorescence with dominantly MD character at 16 938 cm^{-1} and 16 842 cm^{-1} establish the Γ_3 and Γ_1 components of the $^7F_1$ multiplet at 333 cm^{-1} and 429 cm^{-1}, respectively. The components of the $^7F_2$ multiplet are found as $\Gamma_2(1)$ (889 cm^{-1}), Γ_3 (976 cm^{-1}), $\Gamma_2(2)$ (1152 cm^{-1}) and Γ_1 (1175 cm^{-1}). All $^7F_3$ components are identified as $\Gamma_2(1)$ (1859 cm^{-1}), $\Gamma_3(1)$ (1873 cm^{-1}), Γ_1 (1902 cm^{-1}), $\Gamma_3(2)$ (1954 cm^{-1}) and $\Gamma_2(2)$ (2038 cm^{-1}). The four strong lines observed in the $^5D_0$–$^7F_4$ fluorescence (14 200–14 700 cm^{-1}) fix the $\Gamma_3(1)$ (2813 cm^{-1}), $\Gamma_2(1)$ (2905 cm^{-1}), $\Gamma_2(2)$ (2979 cm^{-1}) and $\Gamma_3(2)$ (3012 cm^{-1}) components of the $^7F_4$ multiplet. The weak σ-MD transitions observed at 14 664 cm^{-1} and 14 400 cm^{-1} place the two Γ_1 components at 2608 cm^{-1} and 2871 cm^{-1}, respectively. The $\Gamma_1(3)$ component of this multiplet is placed at 3081 cm^{-1} on the basis of the observed $^5D_1$–$^7F_4$ fluorescence line at 15 940 cm^{-1} and $^5D_2$–$^7F_4$ fluorescence lines at 18 373 and 18 436 cm^{-1}. The $^5D_0$–$^7F_5$ fluorescence excited by the dye laser lasing at 16 938 cm^{-1} establishes the positions of the $\Gamma_2(1)$, $\Gamma_3(1)$, $\Gamma_3(2)$ and $\Gamma_3(3)$ components of the $^7F_5$ multiplet at 3786 cm^{-1}, 3799 cm^{-1}, 4000 cm^{-1} and 4052 cm^{-1}, respectively. The $^5D_1$–$^7F_5$ and $^5D_2$–$^7F_5$ fluorescence is rather weak and complex. It has, however, been possible to determine from these fluorescence groups, the positions of $\Gamma_1(1)$ and $\Gamma_1(2)$ components of the $^7F_5$ multiplet at 3844 cm^{-1} and 4008 cm^{-1}, respectively. The remaining one component each of Γ_1 and Γ_2 representations of this multiplet could not be established.

The results of these assignments are summarised in table 2 along with the calculated results. This table gives the experimental and the calculated positions and symmetry

Table 2. Observed and calculated positions of the Stark levels of $Eu^{3+}:LiYF_4$.

	CG (cm^{-1})				Stark level (cm^{-1})		
Multiplet	Observed	Calculated[a]	Calculated[b]	Symmetry	Observed	Calculated[c]	Calculated[d]
$^7F_0$	0	0	0	Γ_1	0	0	0
$^7F_1$	365	369	379	Γ_3	−32	−36	−32
				Γ_1	64	73	63
$^7F_2$	1034	1017	1043	$\Gamma_2(1)$	−145	−157	−146
				Γ_3	−58	−33	−57
				$\Gamma_2(2)$	118	106	116
				Γ_1	141	115	144
$^7F_3$	1922	1856	1899	$\Gamma_2(1)$	−63	−50	−61
				$\Gamma_3(1)$	−49	−35	−48
				Γ_1	−20	−10	−21
				$\Gamma_3(2)$	32	14	31
				$\Gamma_2(2)$	116	105	117
$^7F_4$	2899	2816	2876	$\Gamma_1(1)$	−291	−294	−292
				$\Gamma_3(1)$	−86	−82	−84
				$\Gamma_1(2)$	−28	−39	−23
				$\Gamma_2(1)$	6	−10	3
				$\Gamma_2(2)$	80	68	77
				$\Gamma_3(2)$	113	128	111
				$\Gamma_1(3)$	182	187	179
$^7F_5$	3948	3846	3922	$\Gamma_2(1)$	−162	−167	−162
				$\Gamma_3(1)$	−149	−140	−150
				$\Gamma_1(1)$	−104	−104	−102
				$\Gamma_3(2)$	52	13	47
				$\Gamma_1(2)$	60	66	60
				$\Gamma_1(3)$	—	73	63
				$\Gamma_3(3)$	104	118	110
				$\Gamma_2(2)$	—	145	125
$^5D_0$	17 271	17 234	17 229	Γ_1	0	0	0

assignments of all Stark levels of Eu^{3+} in $LiYF_4$ which have been established in this work.

4. Theory and calculations

The 4f electrons which are responsible for the chemical and spectroscopic properties of the lanthanides [7] are substantially screened by the $5s^2$ and $5p^6$ electrons and hence are weakly perturbed by the ligands in molecular and solid complexes. In fact, the spin–orbit and residual Coulomb interactions for trivalent lanthanides are usually much larger than the ion–ligand interaction. These circumstances allow the crystal field to be treated as a perturbation over the free-ion interactions. In this conventional two-stage approach for the interpretation of the rare-earth spectra in a crystalline environment, the first stage is to solve the free-ion Hamiltonian in order to obtain the free-ion energy levels and wavefunctions. The matrix elements for the residual Coulomb and spin–orbit

Table 2. *continued*

	CG (cm^{-1})				Stark level (cm^{-1})		
Multiplet	Observed	Calculated[a]	Calculated[b]	Symmetry	Observed	Calculated[c]	Calculated[d]
$^5D_1$	19 028	19 002	19 043	Γ_3	−7	−12	−12
				Γ_1	15	23	24
$^5D_2$	21 502	21 446	21 535	$\Gamma_2(1)$	−52	−29	−28
				Γ_1	−23	−9	−10
				Γ_3	18	11	13
				$\Gamma_2(2)$	41	17	14
$^5L_6$[e]	—	25 280	25 157	$\Gamma_2(1)$	—	−221	−205
				$\Gamma_3(1)$	24 953	−206	−189
				$\Gamma_1(1)$	—	−194	−176
				$\Gamma_2(2)$	25 027	−121	−106
				$\Gamma_2(3)$	—	−115	−102
				$\Gamma_3(2)$	25 241	66	61
				$\Gamma_1(2)$	—	111	97
				$\Gamma_3(3)$	25 415	204	186
				$\Gamma_2(4)$	25 418	206	195
				$\Gamma_1(3)$	—	210	183
RMS deviations		55	24			13	20

[a] Calculated using the following parameters from [3]:

$E^1 = 5544\ cm^{-1}$ $E^2 = 24.83\ cm^{-1}$ $E^3 = 585\ cm^{-1}$ $\zeta = 1285\ cm^{-1}$

$\alpha = 20\ cm^{-1}$ $\beta = -640\ cm^{-1}$ $\gamma = 1750\ cm^{-1}$.

[b] Calculated using our values as follows:

$E^1 = 5549.2\ cm^{-1}$ $E^2 = 24.8\ cm^{-1}$ $E^3 = 585.2\ cm^{-1}$ $\zeta = 1307\ cm^{-1}$

$\alpha = 17.1\ cm^{-1}$ $\beta = -639.4\ cm^{-1}$ $\gamma = 1749.8\ cm^{-1}$.

[c] Calculated using the parameters in set A of table 3.

[d] Calculated using parameters in set B of table 3.

[e] This multiplet was not included in the least-squares analysis. The observed positions of levels rather than splittings are given for this multiplet.

interactions can be written as [7]

$$\langle f^N \tau SL | H_{\text{Coul}} | f^N \tau' S' L' \rangle = \sum_{k=0}^{3} e_k E^k \tag{1}$$

$$\langle f^N \tau SLJ | H_{\text{s-o}} | f^N \tau' S' L' J \rangle = \zeta_{4f} (-1)^{J+L+S'} \begin{Bmatrix} L & L' & l \\ S' & S & J \end{Bmatrix} \sqrt{84} \langle f^N \tau SL \| V^{(11)} \| f^N \tau' S' L' \rangle. \tag{2}$$

Here e_k are the angular parts of the matrix elements and E^k and ζ_{4f} are to be treated as adjustable parameters. The term in the braces is the six-J symbol and $\langle \| V^{(11)} \| \rangle$ are the reduced matrix elements of the unit tensor operator $V^{(11)}$. The treatment in which only the ground-state configuration ($4f^N$) is considered usually leads to substantial discrepancies between the calculated and the experimentally estimated positions of the free-ion energy levels. The dominant part of the configuration interaction via the

Coulomb field can be included by adding the following terms to the diagonal matrix elements of the free-ion matrices:

$$\delta(\psi, \psi')[\alpha L(L+1) + \beta G(G_2) + \gamma G(R_7)]. \tag{3}$$

Here, $G(G_2)$ and $G(R_7)$ are the eigenvalues of the Casimir operators for the groups G_2 and R_7 used to classify the states of the $4f^N$ configuration; α, β and γ are the radial parameters to be adjusted. The configuration interaction via the spin–orbit interaction simply screens the spin–orbit coupling radial integrals and is automatically taken care of by parametrisation of the spin–orbit interaction. We could not consider the remaining interactions such as spin–other-orbit, owing to insufficient experimental data.

The combined energy matrices for the Coulomb, the spin–orbit and the configuration interactions were constructed for each J-value of the $4f^6$ configuration of Eu^{3+}. Since we have no experimental data for the multiplets with J greater than 6, our calculations are restricted to $J = 0$–6 only. The sizes of the free-ion energy matrices were large, requiring a huge amount of data to be fed into the computer to build up these matrices. We checked the correctness of our programming procedure and matrices by comparing some of our results with those applicable to Eu^{3+} in aqueous solutions [8]. There was almost complete agreement in general. However, a few discrepancies exist. Our calculated positions of the $^5D_4$, $^5F_4$ and $^5I_4$ levels are 27 672 cm^{-1}, 33 672 cm^{-1} and 33 893 cm^{-1}, respectively, against the calculated values of 27 670 cm^{-1}, 33 651 cm^{-1} and 33 914 cm^{-1} in reference [8]. We checked our programs and energy matrices several times but could not find any reason for this discrepancy.

The experimental estimates of the free-ion levels were obtained from the centres of gravity (CGs) of the observed positions of the Stark components of a given multiplet. Only those multiplets (except $^7F_5$) for which all the components could be identified were considered for the theoretical analysis. The positions of the ^7F_J ($J = 0$–4) and ^5D_J ($J = 0$–2) multiplets are well established from our experimental results. The calculated positions of the missing $\Gamma_1(3)$ and $\Gamma_2(2)$ Stark levels of the $^7F_5$ multiplet were used to estimate its CG. The large size of the free-ion matrices for Eu^{3+} makes any minimisation exercise impractical (and expensive) and we had to resort to an approximate procedure to reduce the discrepancies between the experimentally estimated and the calculated energies of the free-ion levels. We started with the free-ion parameters of [3]. The starting parameters gave an RMS deviation of nearly 55 cm^{-1}. The free-ion parameters were changed one at a time in small steps and the RMS deviation was calculated in each step. Thus for each parameter the minimum RMS deviation and the corresponding value of the parameter were obtained. Using this procedure we could reduce the RMS deviation to 24 cm^{-1}. Somewhat different procedures were also adopted but the RMS deviation changed only slightly. These parameters were then used to obtain the zero-order wavefunctions to carry out the crystal-field calculations.

5. Crystal-field calculations

The crystal-field Hamiltonian [7] can be expanded in terms of the spherical tensor operators $C_q^{(k)}$:

$$V = \sum_{k,q,i} B_q^k (C_q^{(k)})_i. \tag{4}$$

Here summation involving i is over all the electrons of the ion of interest. The matrix elements of the odd crystal-field terms (i.e. k odd) between states of the same configuration vanish because these states have the same parity. However, the odd terms are responsible for the forced ED transitions between the states of the $4f^N$ configuration by mixing into it the states of configurations of opposite parity [9]. The term with $k = q = 0$ shifts the configuration as a whole and does not contribute to the splittings within a configuration and hence can be neglected in the first approximation. Thus the crystal-field Hamiltonian for the Eu^{3+} ion in S_4 point symmetry can be written as

$$V = \sum_{k=2,4,6} B_0^k(C_0^{(k)}) + \sum_{k=4,6} [B_4^k(C_4^{(k)} + C_{-4}^{(k)}) + iB'^k_4(C_4^{(k)} - C_{-4}^{(k)})]. \quad (5)$$

In this notation all the seven parameters are real. Of these seven parameters, the axial parameters with $q = 0$ are independent of the choice of x and y axes of the coordinate system, while the remaining four parameters ($q \neq 0$) depend on the choice of the coordinate system. The choice of the z axis is dictated by the crystal symmetry axis (c axis); no unique choice exists for the x and y axes. A proper choice of the rotation angle ϕ about the z axis which leaves the axial parameters unchanged [10] can be used to make one of the remaining parameters zero, so that we need to determine only six parameters. In the calculations presented here, we have arbitrarily set $B_4'^4$ to zero. Of the two degenerate irreducible representations Γ_3 and Γ_4, only one needs to be considered as far as the crystal-field calculations are concerned. The Jz bases for the representations Γ_1, Γ_2 and Γ_3 are (0, ±4), (±2, ±6) and (1, −3, 5), respectively.

The experimental values of the crystal-field splittings were obtained by taking the differences of the Stark components of a given multiplet with respect to its lowest Stark component. In this manner, a total of 23 such energy differences (excluding reference levels) were obtained, 19 belonging to the ^7F_J (J = 0–5) multiplets and four to the ^5D_J (J = 0–2) multiplets. We did not include the $^5L_6$ multiplet for the optimisation of parameters because of lack of sufficient experimental data on this multiplet.

The crystal-field energy matrices for the three representations Γ_1, Γ_2 and Γ_3 were constructed for each multiplet neglecting matrix elements between the different J multiplets. The starting parameters, taken from [3], gave an RMS deviation of 23 cm^{-1} and 25 cm^{-1}, respectively, for the 19 and 23 energy differences mentioned above. A least-squares analysis reduced the RMS deviations to 17.5 cm^{-1} and 20 cm^{-1}, respectively. A repetition of these calculations using a totally random set of starting parameters did not modify the RMS deviation and the values of the axial parameters. However, some of the non-axial parameters changed their sign. It was felt that the relatively large RMS deviations obtained in these calculations are due to neglect of J–J mixing effects. We therefore have attempted a limited J–J mixing calculation.

A detailed consideration of the J–J mixing effects in $LiYF_4$:Eu^{3+} requires solving large energy matrices (up to 761 × 761). This is a rather difficult task. The crystal-field energy matrices for the lower ^7F_J (J = 0–6) multiplets and upper ^5D_J (J = 0–3), $^5G_4$, $^5G_5$ and $^5L_6$ multiplets were constructed separately. We had to solve four complex matrices of size 12 × 12 and two of size 13 × 13. To facilitate comparison of the calculated and observed crystal-field splittings, free-ion eigenvalues were appropriately added to the diagonal matrix elements. The least-squares analysis was carried out by taking the lowest Stark component of each multiplet as reference. The starting parameters taken from [3] gave the RMS deviations of nearly 5 cm^{-1} for 19 energy differences corresponding to ^7F_J (J = 0–5) multiplets and nearly 14 cm^{-1} for 23 energy differences when ^5D_J (J = 0–2) multiplets were also included. The six-parameter least-squares fit could bring these

Table 3. Crystal-field parameters. Sets A and B correspond to the best-fit parameters with and without *J–J* mixing for 23 energy differences.

	Set A	Set B
B_0^2 (cm^{-1})	360.5 (±0.2)	370.5 (±2.2)
B_0^4 (cm^{-1})	−723.2 (±0.5)	−821.3 (±3.8)
B_0^6 (cm^{-1})	−42.62 (±0.4)	−81.45 (±3.8)
B_4^4 (cm^{-1})	−929.7 (±0.1)	−1001.0 (±2.9)
B_4^6 (cm^{-1})	−808.8 (±0.1)	−816.0 (±2.6)
$iB_4'^4$ (cm^{-1})	0	0
$iB_4'^6$ (cm^{-1})	238.4 (±0.5)	272.5 (±8.4)
RMS deviation (cm^{-1})	13.1	20.1

RMS deviations to 2.9 cm^{-1} and 13.1 cm^{-1}. Table 2 shows experimental and calculated splittings and table 3 gives the corresponding crystal-field parameters.

We notice a considerably improved agreement for the low-lying ^7F_J multiplets, thus establishing the fact that the *J–J* mixing effects are quite important for these closely spaced multiplets. The agreement for higher multiplets (^5D_J) is, however, poor even when *J–J* mixing effects are included. A similar discrepancy has been reported under a somewhat different truncation procedure [11]. The mixing of ^3P states, which was neglected in [11], was suggested as a possible cause for this disagreement. However, our calculations rule out this possibility as we have used intermediate wavefunctions, which take account of these effects to a certain extent. Taking the $^2H_{11/2}$ multiplet of Nd^{3+} as an example, Faucher *et al* [12] have recently demonstrated the inadequacy of the conventional crystal-field theory for coupled states (i.e. states having the same *S*-, *L*- and *J*-values). The ^5D_J multiplets involve coupled states. We have no satisfactory explanation for the poor agreement for the ^5D_J multiplets. We, nevertheless, feel that more exact *J–J* mixing calculations covering larger experimental data should be attempted.

6. Summary and conclusions

We have recorded absorption and laser-induced fluorescence spectra of $LiYF_4:Eu^{3+}$ in σ, π and axial modes of polarisation at liquid-nitrogen temperature. Some of the spectral lines show a pure MD character, while some others have a pure ED character. There are still others which show a mixed character. It is interesting to point out that some of the MD transitions ($^5D_0$–$^7F_1$ for example) are among the strongest observed lines for this system. Detailed analysis based on the observed polarisation and other aspects of spectral lines confirms that the relevant Eu^{3+} site symmetry is S_4. We have identified the complete Stark structure of the $^5D_2$ multiplet and the partial structure of the $^5L_6$ multiplet for the first time. In addition, complete assignment of the Stark structure of ^7F_J (J = 0–4), $^5D_0$ and $^5D_1$ multiplets has been made. The $^7F_5$ multiplet has been partially identified. Our experimentally inferred positions of the Stark levels belonging to the ^7F_J (J = 0–4) and $^5D_{0,1}$ multiplets are by and large in agreement (within ±3 cm^{-1}) with those reported by Görller-Walrand *et al*. However, some discrepancy exists for the structure of the $^7F_5$ multiplet. For example, our analysis of the experimental data would place the $\Gamma_2(1)$ and

$\Gamma_3(1)$ levels of the $^7F_5$ multiplet at 3786 cm^{-1} and 3799 cm^{-1}, respectively, compared with 3795 cm^{-1} and 3807 cm^{-1} reported by Görller-Walrand *et al*. The $^7F_4(\Gamma_1(3))$, $^7F_5(\Gamma_1(1))$ and $^7F_5(\Gamma_1(2))$ Stark levels which could not be established by Görller-Walrand *et al* have been identified in this work. At the same time we have failed to observe the $^7F_5(\Gamma_2(2))$ level at 4070 cm^{-1}. The structure of the $^7F_6$ multiplet could not be established as, although we observed the $^5D_2$–$^7F_6$ fluorescence, it was rather weak. It would be necessary to use a sample with a higher Eu^{3+} concentration to establish the structure of this multiplet. A theoretical interpretation of the spectroscopic data in terms of a Hamiltonian consisting of the free-ion and crystal-field interactions has been attempted. Rigorous calculations for Eu^{3+} with six electrons in the 4f shell are difficult to make. A proper least-squares analysis of the free-ion energy levels was not possible. An approximate procedure gave an RMS deviation of 24 cm^{-1} for the nine multiplets investigated in the present work. Our crystal-field calculations show that *J–J* mixing effects are quite important for this ion. A calculation of crystal-field splittings including limited *J–J* mixing effects gave an RMS deviation of 13 cm^{-1} for 32 Stark levels belonging to the ^7F and ^5D multiplets. Under these conditions the RMS deviation for the $^7F_{0-5}$ multiplets is about 3 cm^{-1}.

References

[1] Bihari B 1988 *PhD Thesis* Indian Institute of Technology, Kanpur
[2] Sharma K K and Erickson L E 1985 *J. Phys. C: Solid State Phys.* **18** 2935
[3] Görller-Walrand C, Behets M, Porcher P, Moune-Minn D K and Laursen I 1985 *Inorg. Chim. Acta* **109** 83
[4] Thoma R E, Weaver C F, Friedman H A, Insley H, Harris L A and Yakel H A 1961 *J. Chem. Phys.* **65** 1096
[5] Koster G F, Dimmock J O, Wheeler R G and Statz H 1963 *Properties of the Thirty-two Point Groups* (Cambridge, MA: MIT)
[6] Morrison C A and Leavitt R P 1982 *Handbook on the Physics and Chemistry of Rare Earths* vol 5, ed K A Gschneidner and L Eyring (Amsterdam: North-Holland) pp 461–692
[7] Wybourne B G 1965 *Spectroscopic Properties of Rare Earths* (New York: Wiley)
[8] Carnall W T, Fields P R and Rajnak K 1968 *J. Chem. Phys.* **49** 4450
[9] Judd B R 1962 *Phys. Rev.* **127** 750
[10] Rudowicz C 1985 *Chem. Phys.* **97** 43
[11] Hölsa J and Porcher P 1981 *J. Chem. Phys.* **75** 2108
[12] Faucher M, Garcia D, Caro P, Derouet J and Porcher P 1989 *J. Physique* **50** 219